

## SILANE COVERED MAGNETITE PARTICLES. PREPARATION AND CHARACTERISATION

A. Durdureanu-Angheluta,<sup>a,b</sup> R. Ardeleanu<sup>a</sup>, M. Pinteala<sup>a\*</sup>,  
V. Harabagiu<sup>a</sup>, H. Chiriac<sup>c</sup>, B. C. Simionescu<sup>a</sup>

<sup>a</sup>“Petru Poni” Institute of Macromolecular Chemistry, 700487 Iasi, Romania

<sup>b</sup>“Gh. Asachi” Technical University, 700050 Iasi, Romania

<sup>c</sup> National Institute of Research and Development in Technical Physics, 700050 Iasi

Nanosized magnetic particles are well known for their ability to perform ionic exchange, to specifically coordinate different organic ligands, to selectively transport cells and other nanometric entities. The work describes the preparation of organic-inorganic stable magnetic particles with dimensions of hundred of nanometers through the interaction between magnetite particles and different organothriethoxysilanes ( $\text{RSi}(\text{OC}_2\text{H}_5)_3$ ; R: methyl, allyl, 3-aminopropyl). The particles were prepared in two steps: (a) co-precipitation of the  $\text{Fe}^{2+}/\text{Fe}^{3+}$  system in amoniacal solutions and (b) condensation of hydroxyl surface groups of magnetite with silane monomers. The dimensional distribution of magnetite particles was reduced while the dimension of the particles was increased from cca 250 nm in magnetite to cca 500 nm after the treatment with silanes. Covering of magnetite particles with silanes induces a decrease of the magnetization from 64 emu/g to 22-56 emu/g depending on silane nature.

(Received March 22, 2008; accepted March 27, 2008)

*Keywords:* Magnetic particles, Magnetite, Silane, Co-precipitation

### 1. Introduction

Nanotechnology represents a new phase of knowledge and technical development with potential applications in various areas such as electronics, chemistry, metallurgical engineering, mechanics [1]. In the near future the nano sized high performance materials and new production processes based on nanotechnology will offer opened roads for new knowledge-based applications [2].

Nanotechnologies development is related to the improving of different theoretic aspects in nanosciences and to the preparation of new nanomaterials able to support the development of some new applications. For nanomaterials, submicron sizes are essential but within a larger approach all the materials with characteristic properties determined by dimension, structure, methods and nanotechniques can be included in nanomaterials field.

Much attention has been paid to the preparation of nanocrystalline materials with application in energetics (solar energy conversion), medicine (drug delivery), electronics (piezoelectric materials, micro laser) [3]. Composite nanoparticles, that, beside magnetic properties, present some characteristics useful in physical and chemical processes like ionic exchange, specific complexation, biocompatibility and bioactivity, capacity of selecting and carrying cells and chemical substances, are very important for nanotechnology development [4].

The structure of magnetic particles contains substances with pronounced magnetic properties (iron, iron oxides - magnetite, ferrites). Magnetic particles present a high magnetic

---

\* Corresponding author: pinteala@icmpp.ro

moment and can be used as nonmagnetic entities carriers (cells, active biologic substances, antibodies, enzymes, nucleic acids, drugs, xenobiotics) in external magnetic environments.

Due to this property the magnetic particles are promising for many researchers in biological sciences [5].

Magnetic particles can be also used as magnetic fluids, catalytic agents and ceramics, for information storage, light - emitting diodes, pigments in paints and cosmetics [6, 7].

Magnetite ( $\text{FeO}\cdot\text{Fe}_2\text{O}_3$ ), the most useful magnetic nanomaterial, has an inverse spinel cubic structure, the oxygen atom forms a closed packing, and the iron cations take up the interstitial tetrahedral or octahedral positions. Electrons can jump from  $\text{Fe}^{2+}$  to  $\text{Fe}^{3+}$  at room temperature [8]. These magnetic nanoparticles can be dispersed in proper solvents forming homogenous suspension called ferrofluids after their surface is coated [9].

The magnetic fluids can be hydrophobic or hydrophilic based on non-wetted or absorbent groups on the particles surface.

The magnetite surface can be grafted with monomers or polymers (covalent bonds) or can be modified by adsorption, electrostatic interaction, hydrogen bonding or by other types of interaction with stabilizers in order to obtain stable particles [10]. Some of these stabilizers (surfactants or polymers) are reacted during the preparation of magnetic particles to avoid their aggregation [11]. The attached covalent monomers, homopolymers or block copolymers must have in their chemical structure organic functions capable of interaction with the hydroxyl groups on particle surface. The most used functional group is the carboxylic one. Poly(methacrylic acid) was recently used for magnetite stabilization [12].

The literature describes the stabilization of magnetite particles with 3-aminopropyltriethoxysilane [13]. Here, we report the synthesis and characterization of magnetic particles with magnetite core and hydrophilic - aminic groups - or hydrophobic - allyl and methyl groups shell. All these organic groups are covalently linked from magnetite particle with a siloxi spacer. The influence of organic radical bound to Si toward the reaction of magnetite with triethoxysilanes and toward the dimensional polydispersity of the stable particles was investigated.

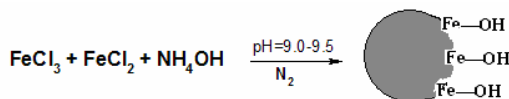
## 2. Experimental

### 2.1. Chemicals

3-aminopropyltriethoxysilane (APTES), allyltriethoxysilane (ATES), methyltriethoxysilane (MTES),  $\text{FeCl}_3\cdot 6\text{H}_2\text{O}$  (Aldrich),  $\text{FeCl}_2\cdot 4\text{H}_2\text{O}$  (Aldrich), HCl 2M (Reactivul-Bucuresti),  $\text{NH}_4\text{OH}$  0.7M (Aldrich), citric acid tripotassium salt ( $\text{C}_6\text{H}_5\text{O}_7\text{K}_3\cdot \text{xH}_2\text{O}$ ), dichloroethane (Reactivul-Bucuresti), dibutyltin dilaurate ( $(\text{CH}_3\text{CH}_2\text{CH}_2\text{CH}_2)_2\text{Zn}[\text{OCO}(\text{CH}_2)_{10}\text{CH}_3]_2$  (Carom-Onesti) were used without advanced purification.

### 2.2. Preparation of magnetite particles (Ma)

The preparation was performed by co-precipitation of  $\text{Fe}^{2+}$  and  $\text{Fe}^{3+}$  ions (Scheme 1) according to the method of Massart [14].



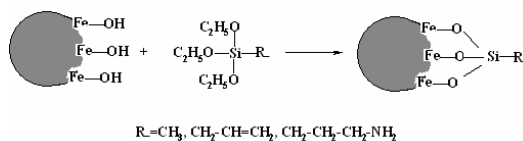
*Scheme 1. Preparation of magnetite particles*

Solutions of 40 ml  $\text{FeCl}_3\cdot 6\text{H}_2\text{O}$  (1M) and 10 ml  $\text{FeCl}_2\cdot 4\text{H}_2\text{O}$ , both prepared in HCl 2M, were added in 500 ml  $\text{NH}_4\text{OH}$  solution (0.7 M) with vigorous stirring and under nitrogen atmosphere, at room temperature. The solution colour changed from orange to black leading to a black precipitate indicating that magnetite was formed. The mixture was kept under stirring during 24 h. 0.553 g citric acid tripotassium salt ( $\text{C}_6\text{H}_5\text{O}_7\text{K}_3\cdot \text{H}_2\text{O}$ ) was then added (molar ratio of citric

acid tripotassium salt to metal species ( $\text{Fe}^{2+} + \text{Fe}^{3+}$ ), 15%). The precipitate was isolated by centrifugation and washed twice with distilled water, then dried at  $65^{\circ}\text{C}$  under vacuum for 24h. The dry magnetite was kept in a desiccator on calcium chloride to avoid the oxidation to maghemite.

### 2.3. Preparation of hydrophilic or hydrophobic magnetic particles

The magnetite particles were functionalized with 3-aminopropylsiloxi (APSO), alylsiloxi (ASO) or methylsiloxi (MSO) groups. The reaction is similar for all three types of silane monomers, i. e., 3-aminopropyltriethoxysilane (APTES), alyltriethoxysilane (ATES) and methyltriethoxysilane (MTES) (Scheme 2).



Scheme 2. Preparation of magnetite/silane monomer particles

The functional magnetite particles with APSO, ASO or MSO were prepared in three 100 ml 3-neck flasks, equipped with a reflux condenser, nitrogen inlet tube, dropping funnel, on a thermostated silicone bath. The reactions were performed in inert atmosphere, at dichloroethane reflux temperature ( $81^{\circ}\text{C}$ ). In the first flask 20 ml dichloroethane, 0.3 g dibutyltin dilaurate (condensation catalyst), 0.6367g  $\text{Fe}_3\text{O}_4$  (2.7 mmol) and 4.73 g APTES (21.4 mmol) ( $\text{Fe}_3\text{O}_4\text{:APTES}=1\text{:}8$ ) were added; the content of the second flask was formed from 10 ml dichloroethane, 0.3 g dibutyltin dilaurate, 0.3184g  $\text{Fe}_3\text{O}_4$  (1.4 mmol) and 3.63g ATES (17.8 mmol) ( $\text{Fe}_3\text{O}_4\text{:ATES}=1\text{:}13$ ), while that of the final flask contained 10 ml dichloroethane, 0.3 g dibutyltin dilaurate, 0.3003g  $\text{Fe}_3\text{O}_4$  (1.3 mmol) and 3.58g MTES (20.1 mmol) ( $\text{Fe}_3\text{O}_4\text{:MTES}=1\text{:}15.4$ ). The unreacted solvent and monomers were separated by vacuum distillation on a rotavapor at  $35^{\circ}\text{C}$ . Magnetic particles, washed with small amounts of toluene for the separation of siloxane oligomers resulted during the reaction and with acetone for the separation of condensation catalyst, were dried in vacuum at  $35^{\circ}\text{C}$  for 24 h.

**2.4. Characterization: FT-IR spectroscopic studies** were recorded on a Bruker Vertex 70 spectrometer; **ATG** curves were obtained with a Q-1500 D derivatograph, system F. Paulik, L. Erdey MomBudapest, at a  $10^{\circ}\text{C}/\text{min}$  heating rate; **scanning electron microscopy** (SEM) measurements were carried out on a Tesla BS 343 instrument; **atomic force microscopy** (AFM) images were obtained on a Quesant Q-Scope 350 instrument (silicon nitrate cantilever (NSC 16)) at a frequency of  $170\pm 200$  KHz; **particle size and particle size distribution** were evaluated on a Microtrac Nanotrac 250 Particle Size Analyzer. **The magnetic properties** were investigated with a Lake Shore 7410 vibrating sample magnetometer.

## 3. Results and discussion

Magnetic materials for biomedical application must present biocompatibility, paramagnetism and stability in adequate solutions, according to their hydrophobic or hydrophilic external shell [15]. These „core-shell” magnetic particles (magnetite-3-aminopropyltriethoxysilane (Ma-APTES), magnetite-allyltriethoxysilane (Ma-ATES) and magnetite-methyltriethoxysilane (Ma-MTES)) contain a magnetite core coated with organic or inorganic molecules or with organic-inorganic mixed structures. The shell type confers a hydrophobic or hydrophilic nature to the particle and determines its stability in adequate solvents.

Magnetite particles (Ma) were obtained by co-precipitation of ferric ( $\text{Fe}^{3+}$ ) and ferrous ( $\text{Fe}^{2+}$ ) ions (molar ratio  $\text{Fe}^{3+}/\text{Fe}^{2+}=1/2$ ) at room temperature in an ammonium hydroxide aqueous solution, with stirring, until the pH of the solution reached 9.0-9.5 (Scheme 1). The formation of magnetite particles can be observed through the appearance of a black colour [14]. In the presence of water, the magnetite particles can be oxidized to maghemite ( $\gamma\text{-Fe}_2\text{O}_3$ ) [16].

Magnetite (Ma) Fourier transform infrared spectra (Fig.1) emphasise the presence of Fe-O bond stretching vibrations at  $590\text{ cm}^{-1}$ , a large band around  $3500\text{-}3300\text{ cm}^{-1}$  – assignable to the Fe-OH – and a deformation vibration of the –OH bond at  $1617.25\text{ cm}^{-1}$ .

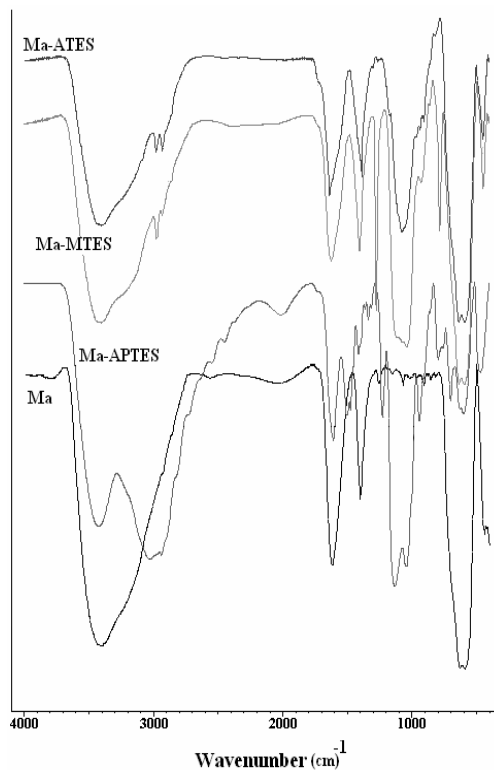


Fig. 1. FT-IR spectra of Ma; Ma-APTES; Ma-ATES; Ma-MTES

The thermogravimetric analysis (Fig. 2) indicates decomposition phenomena in the 50-450 °C temperature interval. The particle is essentially covered by ferroferric hydro- and hydroxyl complexes, as observed through the weight loss (around 20 %, at 150-170 °C, characteristic for water elimination). An easy weight loss (~6 %) around 200-450°C, characteristic for the transformation of ferro-ferric oxide in ferrous oxide [17], is also observed.

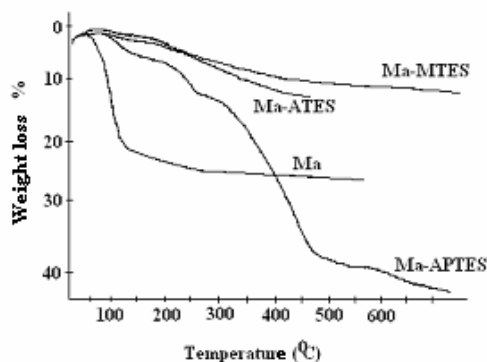


Fig. 2. ATG curves of Ma; Ma-APTES; Ma-ATES; Ma-MTES.

Dimension distribution analysis (Fig. 3a) evidenced the presence of two fractions of particles at 30 nm (12%) and 250 nm (88%). The global dimension of the magnetite particles is estimated to be around 253 nm and the dimensional polydispersity around 1.6-1.7.

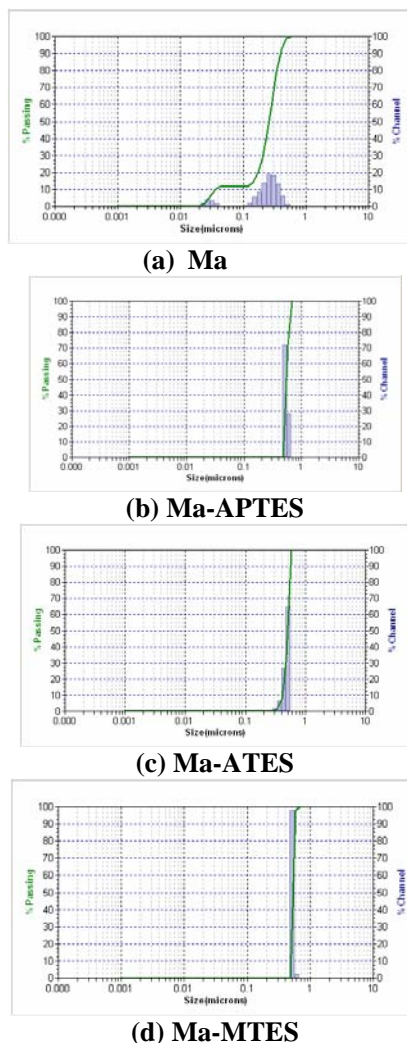


Fig.3. Dimension distribution diagrams of (a) Ma; (b) Ma-APTES; (c) Ma-ATES; (d) Ma-MTES

The surface of magnetite particles was modified by the condensation of hydroxyl groups on the magnetite surface with triethoxy groups of silane compounds (Scheme 2). The condensation reaction is a complex process that depends on experimental conditions (reaction temperature, duration, concentration and functional groups nature of the silane monomers, magnetite surface and dimensional properties, stirring regime, etc.).

Magnetite particles surface was modified with three types of silanes: 3-aminopropyltriethoxysilane (APTES), allyltriethoxysilane (ATES) and methyltriethoxysilane (MTES). These silanes have either absorbent groups (APTES) or non-wetted groups (ATES, MTES) in the structure. The hydrophobic/hydrophilic character of the particles is due to the used monomer.

The FT-IR spectra (Fig. 1) indicate the presence of the covalent bonding of the silane monomer on magnetite surface through the new band at  $1100\text{-}1040\text{ cm}^{-1}$  characteristic for monomer functional groups and for the Si-O-Fe covalent bonds.

In the case of APTES, the absorption band at  $3416\text{ cm}^{-1}$  is characteristic for the free  $\text{NH}_2$ -terminal groups, the band being covered with the stretching vibration band of the  $-\text{OH}$  group. The absorption bands at  $3024\text{-}2933\text{ cm}^{-1}$  and  $1332\text{ cm}^{-1}$  have been associated with the stretching vibration band of  $-\text{CH}_2$  groups and  $\text{C-N}$  bond, respectively, and the bands at  $1223\text{ cm}^{-1}$  and  $938\text{ cm}^{-1}$  were attributed to  $\text{Si-CH}_2$  bond. For ATEES, the FT-IR spectrum indicates the diminishing of the  $-\text{OH}$  characteristic group from Ma and the appearance of the bands in  $2975\text{ cm}^{-1}$  and  $2925\text{ cm}^{-1}$  (allyl groups). The bands at  $1166\text{ cm}^{-1}$  and  $901\text{ cm}^{-1}$  are attributed to the  $\text{Si-C}$  bond. Magnetite particles grafted with MTES present characteristic bands for the  $\text{Si-CH}_3$  bond at  $1272\text{ cm}^{-1}$  and  $927\text{ cm}^{-1}$  and for the  $\text{Si-CH}_2$  bond at  $2969\text{ cm}^{-1}$ .

TGA curves (Fig. 2) indicate an increase of the thermal decomposition process for the modified particles as compared to the uncoated Ma. For magnetite particles, one major decomposition process appears ( $\sim 100\text{ }^\circ\text{C}$ , 20%) and for coated particles an increased number of decomposition processes is noticed. Other phenomena are observed at higher temperatures, besides the decomposition process at  $100\text{ }^\circ\text{C}$ , depending on the grafted organic-inorganic radical (Table 1).

Table 1. Thermo differential analysis data of Ma; Ma-APTES; Ma-ATES; Ma-MTES

Probe Code	Decomposition step	Temperature [ $^\circ\text{C}$ ]	Weight loss [%]
Ma	I	50-150	20
	II	150-450	6
Ma-APTES	I	50-150	4
	II	170-260	5.4
	III	265-450	23
Ma-ATES	I	50-150	1.5
	II	120-250	4.5
	III	250-400	9
Ma-MTES	I	50-150	2
	II	150-250	2
	III	250-450	5

Fig. 4 presents the magnetization curves for the uncoated magnetite and for the three types of grafted particles (Ma, Ma-APTES, Ma-ATES, and Ma-MTES). The saturation magnetization is  $64\text{ emu/g}$  for uncoated magnetite, a value in agreement with literature data [15], while for the coated particles the values are of  $22\text{ emu/g}$  (Ma-APTES),  $56\text{ emu/g}$  (Ma-ATES) and  $55\text{ emu/g}$  (Ma-MTES), respectively. These values suggest that the obtained magnetite is of high quality. The decrease of the magnetization is most likely attributed to the existence of organic-inorganic radicals on  $\text{Fe}_3\text{O}_4$  surface. All these types of particles present a hysteresis phenomena characteristic for ferromagnetic materials [16].

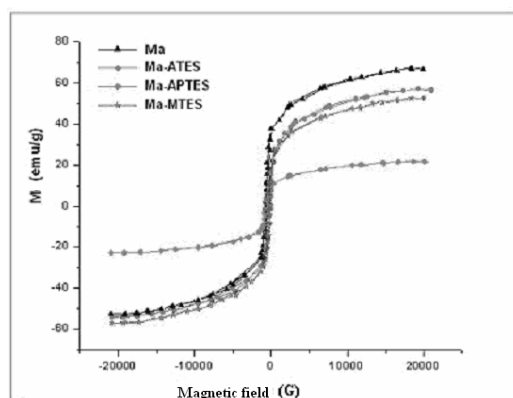


Fig. 4. Magnetization curves for magnetite powder and for magnetite-silane monomer particles

Fig. 3 a-d present the dimensional distributions of magnetite and magnetite-silane monomer particles. Following the modification of magnetite surface (Fig. 3 b,c,d), the magnetite fraction of lower dimensions fully disappears, particles with dimensions around 500 nm (550 nm (Ma-APTES), 496 nm (Ma-ATES), 532 nm (MTES)) and smaller polydispersity ( $\sim 1.1$ ) being formed. This demonstrates again the covering of the magnetite particles with silane monomers. The disappearance of the small fraction of the magnetite particles is due to the crosslinking with three functional silanes.

SEM images (Fig. 5.) shows a self-assembling of the coated particles. SEM images (Fig. 5) and AFM (Fig. 6) images indicate a spherical shape of the magnetite particles before and after the covering with silane monomers [2]. AFM data confirm the SEM and dimension diagram data.

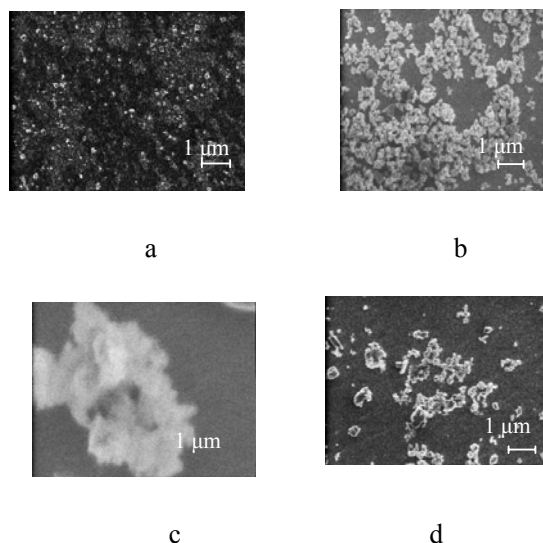


Fig. 5. SEM of the particles: (a) Ma; (b) Ma-APTES; (c) Ma-ATES; (d) Ma-MTES

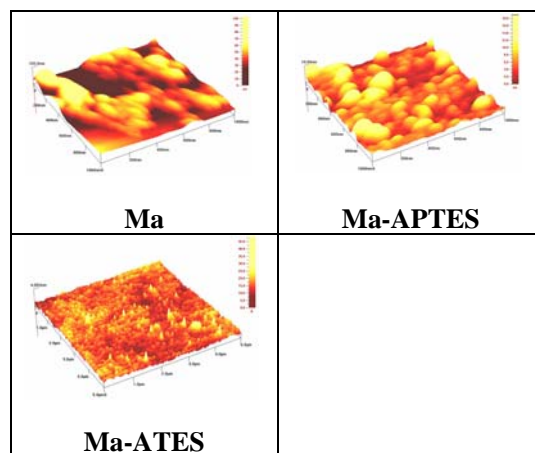


Fig. 6. AFM of Ma; Ma-APTES; Ma-ATES.

#### 4. Conclusions

Magnetic particles of magnetite-silane monomer were prepared by the condensation reaction between OH- groups on the magnetite surface and the ethoxy groups from the silane structure. FT-IR spectra evidence the characteristic band for the Si-O-Fe bond, which demonstrates the covalent bonding of silane groups on magnetite surface. Dimensional distribution analysis, SEM and AFM

indicate the formation of low polydispersity spherical particles of dimensions of hundred of nanometers. The coated magnetite particles dimensions are twice bigger as compared to magnetite, which demonstrates that magnetite surface is grafted with silane monomers. The magnetite particles coated with silane monomers present magnetic properties with potential applications, e.g., as ferrofluids.

### Acknowledgements

This work was supported by The National University Research Council of Romania (Grant CNCSIS GR 64/09.05.2007) Theme I and Theme III and by the CEEEX CICLOMED Project.

### References

- [1] A. Huczko, *Appl. Phys. A* **70**, 365-376 (2000).
- [2] Y. K. Gun'ko, S. C. Pillai, D. Mcinerney, *J. Mat. Sci. Mat. Elec.* **12**, 299-302 (2001).
- [3] Y. Chu, J. Hu, W. Yang, C. Wang, J. Z. Zhang, *J. Phys. Chem. B* **110**, 3135-3139 (2006).
- [4] I. Safarik, M. Safarikova, *Monatshefte fur Chemie* **133**, 737-759 (2002).
- [5] H. H. Yang, S. Q. Zhang, X. L. Chen, Z. X. Zhuang, J. G. Xu, X. R. Wang, *Anal. Chem.* **76**, 1316-1321 (2004).
- [6] A. P. Alivisatos, *Science* **271**, 933 (1996).
- [7] S. Forster, M. Antonietti, *Adv. Mater.* **10**, 195 (1998).
- [8] K. L. Thomas-Keppta, D. A. Bazylinski, J. L. Kirschvink, S. J. Clemett, D. S. McKay, S. J. Wentworth, H. Vali, E. K. Gibson, C. S. Romanek, *Geochim. Cosmochim. Acta* **64**, 4049-4081 (2000)
- [9] X. C. Shen, X. Z. Fang, Y. H. Zhou, H. Liang, *Chem. Lett.* **33**, 1468 (2004)
- [10] J. Dobson, *Febs Lett.* **496**, 1-5 (2001)
- [11] (a) A. Pallandre, K. Glinel, A. M. Jonas, B. Nysten, *Nano Lett.* **4**, 365-371, (2004); (b) L. Bois, A. Bonhomme, A. Ribes, B. Pais, G. Raffin, F. Tessier, *Colloids Surf. A* **221**, 221-230 (2003)
- [12] K. Wormuth, *J. Col. Inter. Sci.* **241**, 366-377 (2001)
- [13] E. Neagu, E. Teodor, G. L. Radu, A. C. Nechifor, *Gh. Nechifor, Rom. Biol. Sci.* **III**, no. 3-4, 1-9 (2005)
- [14] A. Bee, R. Massart, S. Neveu, *J. Magn. Magn. Mater.* **149**, 6-9 (1995)
- [15] P. A. Dresco, V. S. Zaitsev, R. J. Gambino, B. Chu, *Langmuir* **15**, 1945-1951 (1999)
- [16] R. C. Plaza, J. L. Arias, M. Espin, M. L. Jimenez, A. V. Delgado, *J. Col. Inter. Sci.* **45**, 86 (2002)
- [17] A. C. Nechifor, E. Andronescu, *Rom. Biol. Sci.* **III**, no. 1-2, 13-24 (2005)